

³ Illingworth, C. R., "The effects of a sound wave on the compressible boundary layer on a flat plate," *J. Fluid Mech.* **3**, 471-479 (1958).

⁴ Strahle, W. C., "A theoretical study of unsteady droplet burning: Transients and periodic solutions," Princeton Univ. Aeronautical Engineering Lab. Rept. 671 (1963).

⁵ Schlichting, H. and Busmann, K., "Exakte Lösungen für die laminare Grenzschicht mit Absaugung und Ausblasen," *Schriften Deutscher Akad. Luftfahrtforschung* **7**, 25-35 (1953).

Electrode Drops and Current Distributions in an MGD Channel

JOHN J. KARKOSAK*

United Aircraft, Inc., East Hartford, Conn.

AND

MYRON A. HOFFMAN†

Massachusetts Institute of Technology, Cambridge, Mass.

Introduction

THE performance of electrodes in MGD channel flows is of importance in both MGD generator and accelerator applications. It has been predicted by Kerrebrock¹ that large boundary-layer drops may result from a cold electrode wall for the case of equilibrium electrical conductivity. In addition, Podolsky and Sherman² and Hurwitz, Kilb, and Sutton³ have predicted large current concentrations at the corners of both continuous and segmented electrodes. Since these phe-

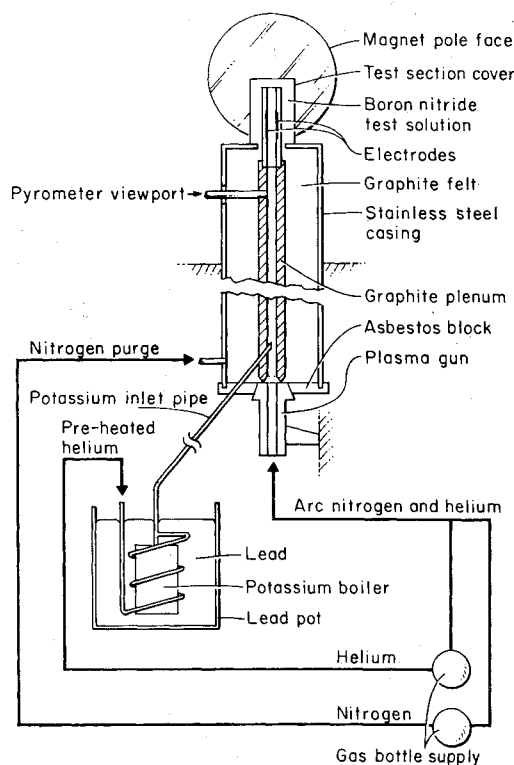


Fig. 1 Schematic diagram of test facility.

Received February 15, 1965. This work was carried out under NASA Grant No. 496 through the Massachusetts Institute of Technology, Center for Space Research.

* Engineer, Advanced Power Systems Group. Student Member AIAA.

† Associate Professor, Department of Aeronautics and Astronautics. Member AIAA.

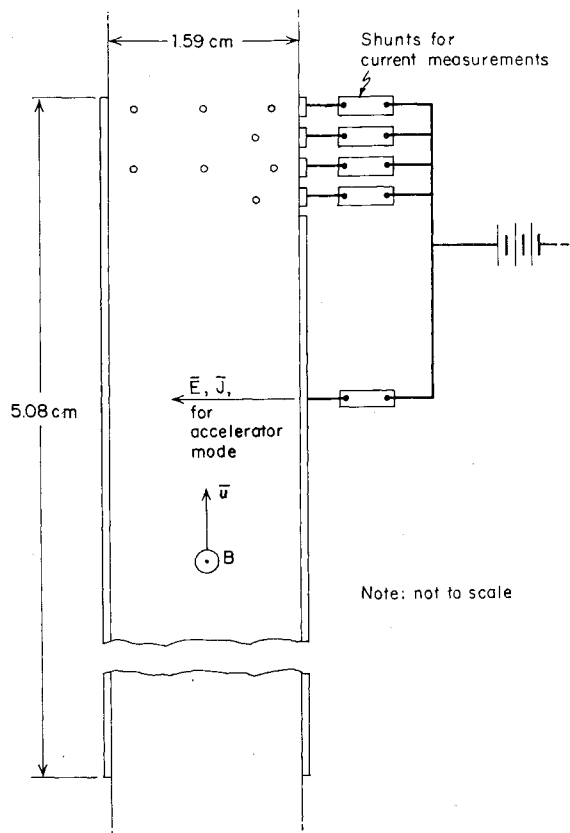


Fig. 2 Schematic diagram of the test section and current measurement circuit.

nomena would seriously limit the performance of MGD generators and accelerators, an experimental investigation is in progress to evaluate their importance. This technical note summarizes the initial results on a continuous electrode geometry.⁴

Experimental Facility and Operating Conditions

The experimental facility shown in Fig. 1 consists of an arc heater and graphite plenum surmounted by a boron nitride test section. The test gas is primarily helium mixed with a nitrogen mole fraction of about 11% to obtain higher gas temperatures. A part of the gas is preheated in a pot of molten lead to about 1000°K. A stainless-steel boiler filled with potassium is immersed in the lead pot and injects approximately 0.3% potassium into the preheated gas stream through a choked orifice. The arc flow and the seeded flow mix in a graphite plenum and then are passed through the test section.

For the tests to be described, the total gas pressure was approximately 1 atm, and the gas temperature as measured by a pyrometer was about 1680°K. The average electrode temperature was found to be 1350°K using a platinum - platinum + 10% rhodium thermocouple attached to the rear of one electrode. The flow velocity calculated from measured flow rates and the gas temperature is estimated to have been about 100 m/sec in the test section.

The test section shown in Fig. 2 has a square cross section of 1.59 cm on a side. It is made of boron nitride and contains one pair of tantalum electrodes with a length to channel height ratio of 3.2. The exit end of one of the electrodes has been subdivided into four small pieces and one large piece, which are electrically insulated from each other by thin boron nitride spacers in the channel wall. However, they are all electrically connected to each other externally after the current-measuring shunts. Using this simple technique, it has been possible to obtain a measure of the current distribu-

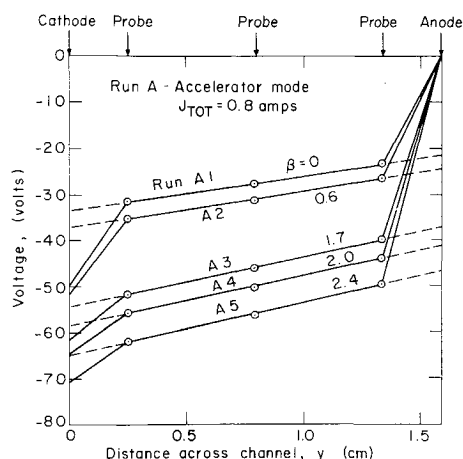


Fig. 3 Potential distribution in plasma between electrodes for accelerator mode of operation.

tion at the exit. Several 0.020-in. tantalum probe wires have been placed across the test section in the direction of the applied magnetic field to measure electrode and plasma potential drops.

An external voltage was impressed on the electrodes and adjusted to result in 0.8-amp total current across the plasma. This total current was maintained constant throughout the runs as the magnetic field was varied from zero to a maximum of 9750 gauss. The magnetic field was maintained in the direction shown in Fig. 2 throughout the experiment. However, experimental data were obtained for both voltage polarities. This provides data with the Lorentz force in both the downstream direction (termed the accelerator mode) and the upstream direction (termed the generator mode).

Experimental Results

Typical potential distributions across the plasma for the accelerator mode are shown in Fig. 3. The results for the generator mode were substantially the same. The constant electric field across the bulk of the plasma indicates reasonably uniform freestream conditions. The electrical conductivity at zero B field has been calculated to be 0.9 mho/m. This is about five times the theoretical value for the estimated freestream composition and temperature and indicates a slightly elevated electron temperature.⁵

As can be seen from Fig. 3, the potential drops near the electrode walls are quite substantial, being on the order of 5 to 40 v. These large electrode drops may actually occur over a distance much smaller than that implied by the straight lines drawn between the data points. It is felt that a better estimate of these drops is obtained by extrapolating the free-

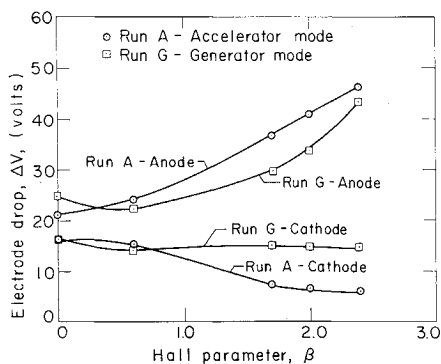


Fig. 4 Variation of electrode voltage drops with Hall parameter for accelerator and generator modes of operation.

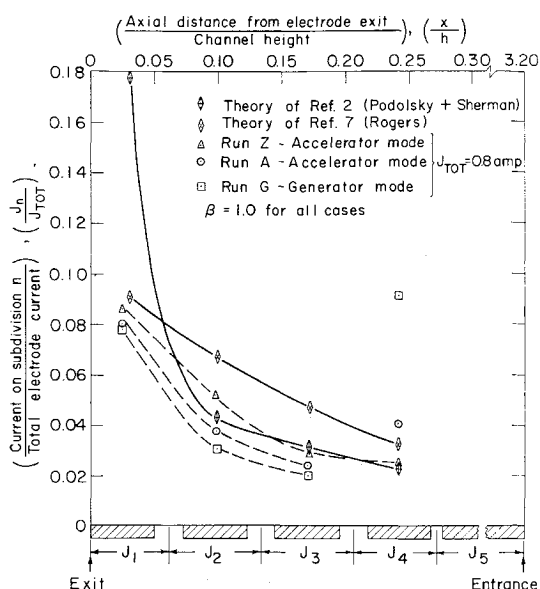


Fig. 5 Current distribution at electrode exit for Hall parameter of 1.0.

stream electric field to the electrode walls as indicated by the dashed lines. These are the values used in Fig. 4.

The effect of increasing magnetic field, or equivalently increasing Hall parameter β on the electrode drops, is shown in Fig. 4. For both modes the anode drop is larger than the cathode drop. In addition, the cathode drop tends to decrease and the anode drop to increase with increasing β . No explanation for this behavior can be offered at this time.

The current concentration at the trailing edge of the subdivided electrode increased somewhat with increasing B field as expected based on results of other experimenters (e.g., Ref. 6), but to a lesser extent than the constant potential theory² predicts. The current distribution that resulted at a Hall parameter of 1.0 (corresponding to a B field of 4000 gauss) is shown in Fig. 5. The four experimental data points for each run represent integrated values of the current over each electrode subdivision. This is indicated by the sketch of the electrode location and size shown on the abscissa. Dashed curves have been used to connect the data points only to facilitate making comparisons. Two of the data points for J_4 fall off the curves. These extraordinarily large currents on subdivision 4 for runs A and G are a consequence of the fact that the current on this subdivision continuously increased during the experiment. No explanation can be offered for this peculiar behavior. Note that in run Z, which preceded runs A and G, the current on subdivision 4 was still "normal."

The theory of Ref. 2 for constant electrode potential and uniform gas properties has been integrated over the appropriate areas for direct comparison with the experimental data. The curves connecting the various points have again been added only to facilitate comparison. As can be seen, the very large current concentration predicted by this theory for the end subdivision (due to a singularity in the theoretical current density at the electrode end) is greatly reduced in actuality.

A modified semiempirical theory by Rogers⁷ which includes a current-dependent electrode potential has also been integrated over the electrode subdivisions and included in Fig. 5. Comparing the shape of this theoretical result with the experimental results indicates that some current-limiting mechanism is present. However, it is not clear whether the observed behavior can be ascribed to a current-dependent electrode drop of the type hypothesized by Rogers. The actual behavior in the electrode drop region is undoubtedly more complex than that included in the theory of either Ref. 2 or 7.

References

- ¹ Kerrebrock, J. L., "Electrode boundary layers in direct-current plasma accelerators," *J. Aerospace Sci.* **28**, 631-643 (1961).
- ² Podolsky, B. and Sherman, A., "Some aspects of the Hall effect in crossed-field MHD accelerators," ARS Preprint 1531-60 (1960).
- ³ Hurwitz, H., Jr., Kilb, R. W., and Sutton, G. W., "Influence of tensor conductivity on current distribution in a MHD generator," *J. Appl. Phys.* **32**, 205-215 (1961).
- ⁴ Karkosak, J. J., "Experimental investigation of exit effects on current distribution in an MGD channel," S. M. Thesis, Massachusetts Institute of Technology (January 1965).
- ⁵ Kerrebrock, J. L. and Hoffman, M. A., "Non-equilibrium ionization due to electron heating," *AIAA J.* **2**, 1072-1087 (1964).
- ⁶ Louis, J. F., Lothrop, J., and Brogan, T. R., "Fluid dynamics studies with a magnetohydrodynamic generator," *Phys. Fluids* **7**, 362-374 (1964).
- ⁷ Rogers, J. W., "A theoretical investigation of the inlet current distribution in an MHD channel," E.A.A. Thesis, Massachusetts Institute of Technology (June 1964).

Expansion of a Finite Mass of Gas into Vacuum

C. GREIFINGER* AND J. D. COLE†

The Rand Corporation, Santa Monica, Calif.

SOME years ago, the authors studied the problem of the expansion into vacuum of a finite mass of gas initially at rest and in a uniform state, under the assumptions that the gas is perfect and inviscid. The results for the case of plane flow appear in Ref. 1, and those for cylindrical and spherical flow are unpublished. From time to time we have, upon request, privately communicated some of the results, together with assurances of the eventual publication of the results in their entirety. However, the continued passage of time has tended to diminish the conviction of these assurances. It therefore seems advisable, at this time, at least to summarize the contents of Ref. 1, and to provide perhaps the most useful result of our unpublished calculations.

We considered the three cases of plane, cylindrical, and spherical symmetry. The flow in the plane case can be described² as the interaction of two expansion fans, or simple waves, centered about the edges ($\pm x_0$) of the initial mass of gas. The x, t plane, or the flow at any time t , is thus divided into two essential regimes, a simple wave and an interaction region. In the cylindrical and spherical cases, the regions of the r, t plane are essentially the same, although pure simple waves no longer exist. In all cases, the flow at any point consists first of the outward motion caused by the expansion fan from the nearest boundary, and then a weakening of this process by the arrival of the expansion fan from the other boundary (plane case) or a reflection from the center (cylindrical and spherical cases).

In the case of plane flow, we constructed, by standard methods,² an exact analytic solution valid for all t . The cylindrical and spherical cases, however, are not amenable to such a treatment. However, since all of the gas eventually

Received February 15, 1965. Any views expressed in this paper are those of the authors. They should not be interpreted as reflecting the view of The Rand Corporation or the official opinion or policy of any of its governmental or private research sponsors. Papers are reproduced by The Rand Corporation as a courtesy to members of its staff.

* Physicist, Physics Department.

† Consultant; also Professor of Aeronautical Engineering, California Institute of Technology, Pasadena, Calif.

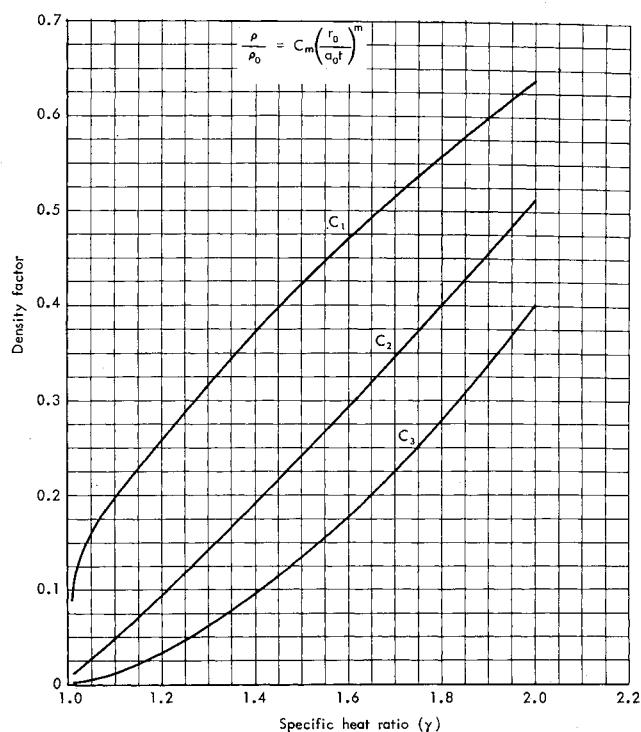


Fig. 1 Asymptotic dependence of density on specific-heat ratio.

enters the interaction region, a solution, asymptotic for large t , in the interaction region provides useful information about the flow. It is precisely such a solution that we constructed by similarity methods.

The principal results of the analysis are 1) the flow velocity $u(r, t)$ is, in all three cases,

$$u(r, t) \cong r/t \quad (1)$$

where r is the distance from the origin; and 2)

$$\rho(r, t)/\rho_0 \cong C_m(\gamma) (r_0/a_0 t)^m \quad (2)$$

$m = 1$ plane case = 2 cylindrical case = 3 spherical case

where ρ_0 is the density, a_0 the sound speed, and r_0 the radius of the initially-uniform gas. The constant in Eq. (2) depends only on m and on the gas constant γ . This solution is asymptotically valid in the region of the r, t plane not too close to the expansion front.

As we mentioned previously, in the case of plane flow an exact analytic solution of the problem can be obtained. By examining this solution in the limit of large t , we were able not only to verify that the assumed similarity solution is, in fact, the asymptotic flow, but we obtained at the same time an analytic expression for the constant $C_1(\gamma)$, viz.,

$$C_1(\gamma) = 2^{\lambda-1} [\Gamma(2\nu - 1)]^{\lambda} / [\Gamma(\nu)]^{2\lambda} \quad (3)$$

where $\lambda = (\gamma - 1)/2$ and $\nu = \frac{1}{2}(\gamma + 1)/(\gamma - 1)$. In Eq. (3), Γ denotes the usual gamma function. In the cylindrical and spherical cases, the asymptotic validity of the similarity solution was established by a numerical integration of the equations of motion. Integration of the equations for different values of γ served to determine the constants C_2 and C_3 as functions of γ . The dependence of C_m on γ for the various cases is shown in Fig. 1.

The results of this study have practical application as an approximation to the expansion of a finite mass of gas into a gas at much lower pressure and density. In this case, a shock wave precedes the expanding gas, but in the limit of ambient vacuum, the effect of the shock wave disappears from the problem. Another application follows from the use